MULTI-ELEMENTAL AND ISOTOPIC CHARACTERIZATION OF COARSE-GRAINED ALLENDE CAIS. F.L.H. Tissot[1], C. Burkhardt[2], G. Budde[2], T. Kleine[2], [1]The Isotoparium, Division of Geological and Planetary Science, Caltech, CA, (tissot@caltech.edu) [2]Institut für Planetologie, University of Münster, Germany.

Introduction: Calcium-Aluminum rich inclusions (CAIs) have long been recognized as the oldest solids in the Solar System, and deciphering the details of their formation and evolution can yield key insights into the earliest formative period of our Solar System. Yet, the processes and conditions under which CAIs formed remain poorly understood. Part of the difficulty stems from the fact that CAIs come in various different flavors and occur as extraneous components in chondrites, *i.e.*, lack "geological" context.

To tease out general features that could shed light on their origins, CAIs have been classified based on numerous criteria, including texture (fine- vs coarse-grained), mineralogy (Type A vs B, [1]), petrographic features (compact vs fluffy), REE patterns (Groups I to V, [2-3]), and isotopic composition (*e.g.*, oxygen). Recently, nucleosynthetic isotope anomalies have been added to this toolbox, and while different types of CAIs are mainly isotopically uniform for many elements, distinct Mo and W isotope signatures suggest that fine- (fg) and coarse- (cg) grained CAIs may have originated from genetically distinct source reservoirs [4-6]. Indeed, while cg-CAIs display only minor (if any) W nucleosynthetic anomalies and virtually constant excess in *r*-process Mo, fg-CAIs display both *s*-process excesses and deficits in Mo and W. This argues against the notion that coarse-grained inclusions formed by melting and recrystallization of their fine-grained counterparts [*e.g.*, 7].

Given the importance of understanding the origin and relation of fine and coarse grained CAIs – in particular with respect to their bearing on the origin of the isotopic dichotomy between non-carbonaceous (NC) and carbonaceous (CC) meteorites [8-9] – we present here results of an ongoing multidisciplinary (petrography, chemistry, isotope composition) study of 9 cg-CAIs from Allende. For all samples, we report REE patterns, Ti, Mo and W nucleosynthetic anomalies, as well as the first mass-dependent W isotope data of cg-CAIs.

Samples: All samples were provided by the Field Museum (Chicago). Seven of the nine CAIs selected are typical coarse-grained Type B CAIs that we identified and extracted from Allende samples. The eighth sample was a slice of the ~1cm diameter inclusion TS45 (a.k.a. ALVIN), which was previously described as a vesicular Forsterite-bearing Type B CAI [10] and whose Al-Mg systematics indicate a time of (re)crystallization ~0.2 Myr after the oldest CAIs [11]. The ninth sample, CG-8, is a compact, irregularly shaped inclusion, with aggregate structure reminiscent of fg-CAIs (sample characterization underway).

Methods: The CAIs were cut out of their host rocks using a wire diamond saw and ethanol as the cutting fluid. Sample surface was cleaned using SiC abrasive paper and/or by gently breaking the CAI in a clean agate mortar, and picking interior pieces only. These CAIs fragments were sonicated for 5 min in dilute HNO_3, MQ and ethanol, prior to powdering in an agate mortar. A small aliquot for major element concentrations measurements by µ-XRF was taken at this point, while the remainder was digested in $HF/HNO_3/HClO_4$ 6:3:0.15 on hot plate at 150°C for 9 days. Resulting solutions were then split in three cuts, one dedicated to Ti, W and Mo nucleosynthetic anomaly analyses, one dedicated to W stable isotope work (using a ^{180}W-^{183}W double spike, [12]) and one aliquot used for concentration work. Elemental purification and isotopic analyses were performed at the Institute für Planetologie in Münster, using well-established methods [13-14], and a Neptune *Plus* MC-ICPMS. Two terrestrial standards were processed along the samples as accuracy monitors.

Results: *REE patterns:* Seven of the 9 inclusions have ~flat REE patterns, typical of cg-CAIs. Of those, the vesicular FoB TS45 is the least REE enriched. CAI CG-7 shows a mainly flat pattern with a slight depletion in Yb. CAI CG-8 displays the highly fractionated Group II pattern, in which ultra-refractory (Tb-Er, Lu) and volatile (Er,Yb) REEs are depleted relative to the moderately refractory REEs (La-Sm, Gd, Tm). This pattern is thought to represent a snapshot in the condensation sequence, after condensation of an ultrarefractory component and before condensation of more volatile REEs [15-17].

Ti anomalies: The Ti isotopic compositions (Fig. 1) of the CAIs are in line with literature data and most samples exhibit anomalies of ~9 ε^{50}Ti. CG-7 and TS45 have lower anomalies of ~6 and ~4 ε^{50}Ti, respectively.

Mo anomalies: Seven of the CAIs exhibit typical *r*-process excess signatures (Fig. 2). In contrast, CG-8 and TS45 are dominated by an *s*-process excess and *s*-process deficit in Mo isotopes, respectively, setting them apart from other coarse-grained inclusions.

W anomalies: Similarly, most CAIs have near-terrestrial ε^{183}W values, in line with previous data [5], except for a minor anomaly in TS45 and an ~1.5 ε^{183}W *s*-process deficit in CG-8.

W mass-dependent fractionation: All CAIs except one plots above the range defined by terrestrial and bulk meteoritic materials (Fig. 3).

Discussion: The data obtained on CG-8 and TS45 reveal that the notion of cg-CAIs having approximately constant Ti, Mo and W nucleosynthetic signatures,

which are distinct (for Mo and W) from those of fine-grained CAIs, is not universal. The *s*-process deficit observed in the Fo-bearing TS45 is also unique for a cg-CAI, and has, so far, only been observed in NC (Non-Carbonaceous) meteorites. The Ti isotope data also places TS45 within the field of bulk meteorites. Considering that TS45 has ~1.5 times lower REE enrichment than typical cg-CAIs, a possible explanation for the non-CAI like isotope signatures could be dilution by non-CAI material during melting and recrystallization. More work will be needed to assess whether or not there is a general trend between REE enrichment and isotopic signatures.

Assuming our classification of CG-8 as a cg-CAI is correct, it would be the first cg-CAI characterized by an *s*-process excess in Mo isotopes, and a $\varepsilon^{183}W$ anomaly. As such, it would open the possibility that some cg-CAIs indeed form by reprocessing of fg-CAIs, and suggest a temporal and/or spatial connection between the mostly separate source reservoirs of fg- and cg-CAIs.

The systematically heavier W stable isotope composition in cg-CAIs relative to bulk planetary materials is consistent with cg-CAIs being evaporation residues. A simple Rayleigh distillation model, starting from a material with chondritic W/Sm ratio, shows that the data can be explained by as little as 3% of W evaporation in vacuum or up to 30% of W evaporation in a low P gas significantly heavier than H_2, and thus possibly oxidizing. This is consistent with the 5-60 % of evaporation derived from Mg and Si isotopes [18].

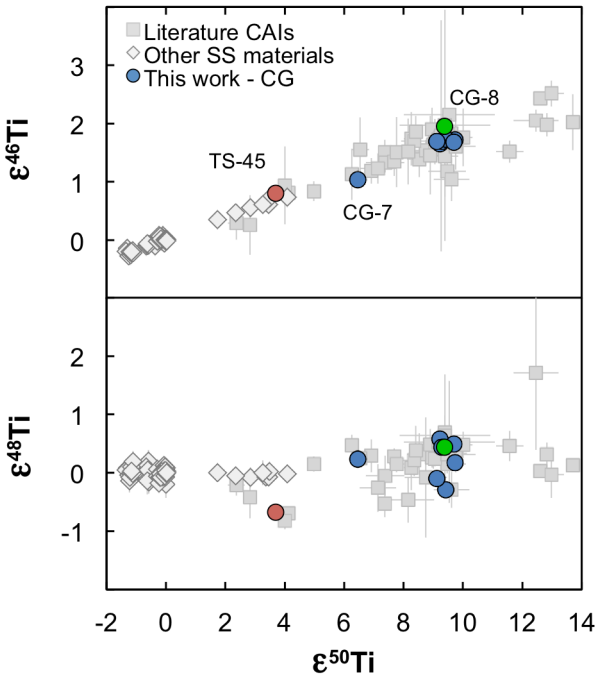

Fig. 1. *Titanium isotope anomalies in the coarse-grained CAIs in this study. Literature data from [19].*

References: [1] Grossman, L. (1975) GCA, 39, 433-&. [2] Tanaka, T., & Masuda, A. (1973). Icarus, 19(4), 523-530. [3] Mason, B. and Taylor, S.R. (1982) *Smithsonian Contr. Earth Sci.*, #25. [4] Burkhardt, C. et al., (2011) *EPSL*, 312, 390-400. [5] Kruijer., T.S. et al., (2014) *EPSL*, 403, 317-327. [6] Brennecka, G. et al., (2018) *LPSC*, abstract #2429. [7] McPherson, G. et al., (2012) *EPSL*, 331-332, 43-54. [8] Warren, P.H. (2011) *EPSL*, 311, 93-100. [9] Budde, G. et al., (2016) *EPSL*, 454, 293-303. [10] Bulloch, E.S. et al., (2012) *MAPS*, 47, 2128-2147. [11] McPherson, G. et al., (2017) *GCA*, 201, 65-82. [12] Krabbe, N. et al., (2017) *Chem. Geol.*, 450, 135–144. [13] Zhang, J. et al., (2011) *JAAS*, 26, 2197. [14] Budde, G. et al., (2018) *GCA*, 222, 284-304. [15] Boynton, W.V. (1975) *GCA*, 39, 569-584. [16] Davis, A., & Grossman, L., (1979) *GCA*, 43, 1611-1632. [17] Kornacki, A.S., & Fegley, B., (1986) *EPSL*, 79, 217-234. [18] Grossman, L. et al., (2008) *GCA*, 72, 3001-3021. [19] Davis, A.M. et al., (2018) *GCA*, 221, 275-295.

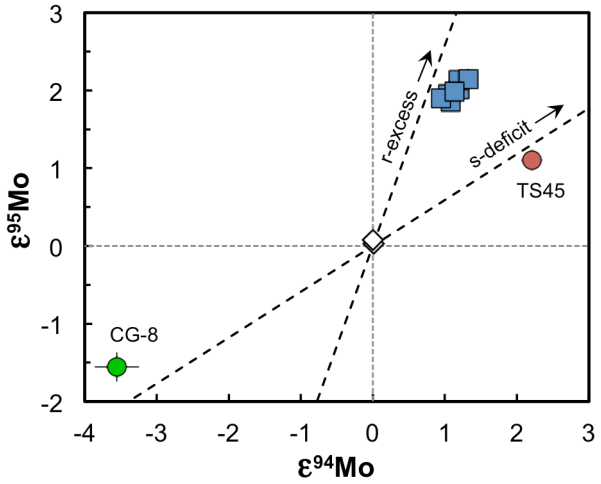

Fig. 2. *Diagram of $\varepsilon^{95}Mo$ vs. $\varepsilon^{94}Mo$ for bulk CAIs from this study. Most CAIs show the typical* r*-process enriched signature (blue squares), while TS45 and CG-8 are dominated by an* s*-process deficit and excess, respectively.*

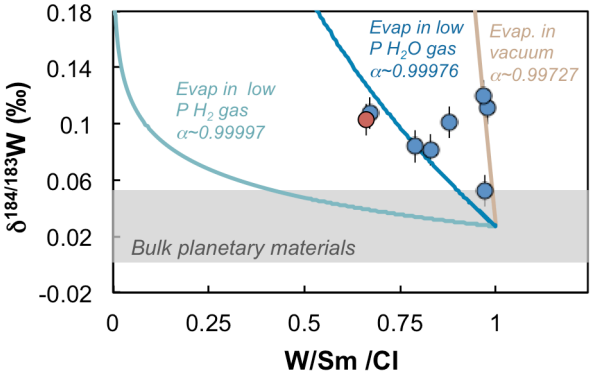

Fig. 3. *W stable isotope data in 8 of the 9 coarse-grained CAIs in this study (CG-8 had too little W to be measured). Solid lines show Rayleigh distillation trajectories during evaporation under different P conditions.*